Low threshold high stability passively mode-locked laser performance of a disordered crystal: $Nd^{3+}:Gd_{0.5}Y_{2.5}Al_5O_{12}$

Chao Feng (冯 超)[1,2], Zhaojun Liu (刘兆军)[2], Zhenhua Cong (丛振华)[2],
Xiaodong Xu (徐晓东)[3], Jun Xu (徐 军)[4], Han Rao (饶 瀚)[2], Fen Bai (白 芬)[5],
Ping Li (李 平)[2], Qingpu Wang (王青圃)[1,2,*], and Jiaxiong Fang (方家熊)[1,2]

[1]*Advanced Research Center for Optics, Shandong University, Jinan 250100, China*
[2]*School of Information Science & Engineering, Shandong University, Jinan 250100, China*
[3]*Jiangsu Key Laboratory of Advanced Laser Material and Device, School of Physics and Electronic Engineering,*
Jiangsu Normal University, Xuzhou 221116, China
[4]*School of Physics Science and Engineering, Institute for Advance Study, Tongji University, Shanghai 200092, China*
[5]*College of Science, China University of Petroleum (East China), Qingdao 266580, China*
Corresponding author: qpwang@sdu.edu.cn

A stable passively mode-locked laser of $Nd^{3+}:Gd_{0.5}Y_{2.5}Al_5O_{12}$ (Nd:GYAG) disordered crystal is experimentally investigated both using Z-type and W-type cavities with a semiconductor saturable absorbed mirror. The continuous-wave mode-locked threshold of the absorbed pump power is just 1.8 W. The maximum average output power is 210 mW, which is obtained at the absorbed pump power of 2.3 W. The pulse width is measured to be 11.1 ps assuming a Gaussian shape.

OCIS codes: 140.3380, 140.3530, 140.4045.
doi: 10.3788/COL201614.111402.

During the past two decades, passively mode-locked (PML) lasers have been studied in depth and have wide applications such as the preparation of materials, optical sensors, information transmission and storage, medical treatment, and optical coherence tomography[1,2]. Compared with other mode-locking techniques, saturable absorber mode locking shows clear advantages (such as self starting, easy operation, and so on)[3]. Recently, two-dimensional materials including graphene, carbon nanotubes (CNTs), transition-metal dichalcogenides (TMDs), topological insulator (TI), and black phosphorus (BP) have been successfully used to achieve such lasers and show a high performance in different wavelength regions[4–16]. However, all the reports showed that the time durations of the stable continuous-wave mode-locked (CWML) laser achieved by the above-mentioned materials were not longer than that of the semiconductor saturable absorbed mirror (SESAM). Nevertheless, the shortest pulse width of such a saturable absorber-based PML laser was still achieved by using the SESAM[17]. Moreover, SESAMs have free designable characteristics that the nonsaturable losses, modulation depth, absorption band, and saturation fluence could be exactly controlled to satisfy the specific requirements of lasers[18]. So far, the SESAM is still the most effective and commonly-used saturable absorber to guarantee the stability of CWML lasers.

Traditional Nd^{3+}-doped crystals (Nd:YAG, Nd:YVO₄, Nd:GGG, etc.) have shown a better performance and have already been employed as the gain media to get PML laser output[19–21]. However, such single crystals have some shortcomings for ultrafast lasers. One is the narrow fluorescence spectral line, which limits the pulse width of the CWML laser. By comparison, the disordered crystals have strong inhomogeneous broadening spectra of both absorption and emission. Nd^{3+}-doped mixed garnets, having the excellent properties like higher thermal conductivity as well as better physical and chemical properties, have better ultrashort laser performance than single garnets. Therefore, a large number of such crystals were prepared and employed to achieve PML laser pulses, including GSAG, GLAG, LYAG, YSAG, CNGG, GSGG, GAGG, LGGG, CLNGG, GYSGG, etc.[22–33]. Additionally, Nd:GYAG was also a typical mixed garnet crystal and was first demonstrated by Di *et al.* in 2011[34]. In the article, the author indicated that the pump efficiency of the continuous wave (CW) laser increases by replacing Lu^{3+} or Y^{3+} ions with large Gd^{3+} ions. Such high efficiency can guarantee reasonable thermal effects. On the other hand, the higher efficiency can also guarantee a lower CWML threshold. Therefore, a stable CW mode-locked laser might be achieved in low incident power level. As the PML laser of Nd:LYAG has been successfully achieved by using an SESAM[26], better performance of an Nd:GYAG PML laser is anticipated.

In this Letter, we present a stable PML laser of a novel disordered Nd:GYAG crystal with a commercial SESAM. First, CW performance of the Nd:GYAG laser was studied. Then, two different resonator cavities were designed to achieve the PML laser. Finally, an 11.1 ps PML laser pulse with a pulse repetition frequency of 88.3 MHz at the absorbed pump power of 2.3 W. The corresponding average output power was 210 mW with the slop efficiency calculated to be 15.5%. The laser exhibited at 1064.4 nm with an FWHM of 0.286 nm.

The laser gain medium of Nd:GYAG was grown by the Czochralski method according to the formula $Nd_{0.03}:Gd_{0.495}Y_{2.475}Al_5O_{12}$. It was a 3 at. % Nd-doped GYAG, cut into a cube and had a dimension of $4\,mm \times 4\,mm \times 5\,mm$. The crystal was coated for AR (antireflection) at both 808 and 1064 nm. Then, it was water cooled at 20°C.

A fiber-coupled 808 nm diode laser was employed as the pump source. The maximum output power of the laser diode pump was about 25 W. The diameter of the fiber was 400 μm and the numerical aperture was about 0.22. Three different resonator cavities were designed respectively.

A 30 mm plano–concave cavity was first used to study the CW laser shown in Fig. 1. M1 was a plano mirror with an AR coating at 808 nm and a high reflection (HR) coating at 1.06 μm. The output coupler (M2, $R = 80$ mm) had a transmission of 4%. By using the ABCD matrix propagation theory and considering the thermal lens effect, the beam waist radii on the Nd:GYAG and the saturable absorber were about 300 and 100 μm, respectively.

As shown in Fig. 2, a 1300 mm Z-type cavity was designed to achieve a CWML laser. Here, M1 is the same as the input mirror mentioned above; the output coupler M3 was also the same as the M2 mentioned above. M2, HR

coated at 1030–1080 nm was concave with a 500 mm curvature radius.

The last cavity for the CWML laser was a W-type cavity with a total length of 1685 mm, as shown in Fig. 3. The input mirror M1 and the output coupler M4 were the same as the mirrors mentioned above. The M2 and M3 were both HR coated at 1030–1080 nm and were concave mirrors with curvature radii of 200 and 800 mm, respectively. By using the ABCD matrix propagation theory and considering the thermal lens effect, the beam waist radii on Nd:GYAG and the saturable absorber were about 150 and 50 μm, respectively. The SESAM was a commercial product (Batop). The modulation depth was 3% and the relaxation time was 500 fs. The power meter was a Molectron PM30-type probe and a Molectron EPM2000 meter. The waveform was detected by a 1 GHz InGaAs detector produced by New Focus. It has a rising time of 400 ps. The oscilloscope was produced by Agilent (8 GHz, DSO90804A).

First, the CW laser output performance of the Nd:GYAG was studied. The output power versus the absorbed pump power is shown in Fig. 4. The oscillation threshold of the CW laser was below 0.8 W. A 1.6 W maximum output power was measured at the absorbed
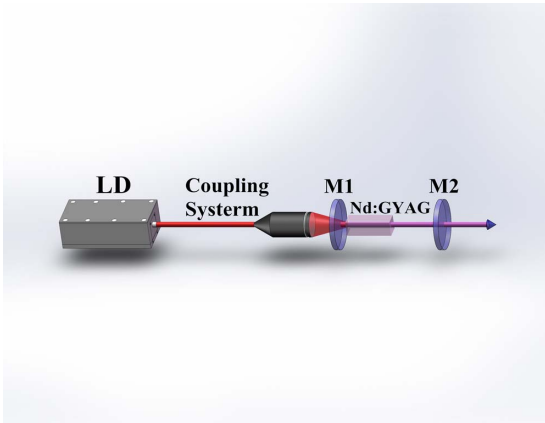

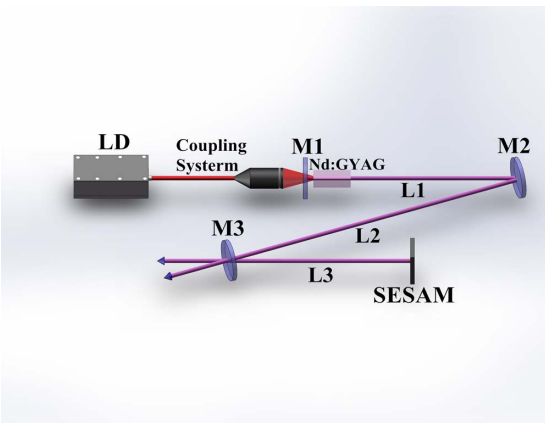Fig. 1. Diagram of CW laser experimental setups.

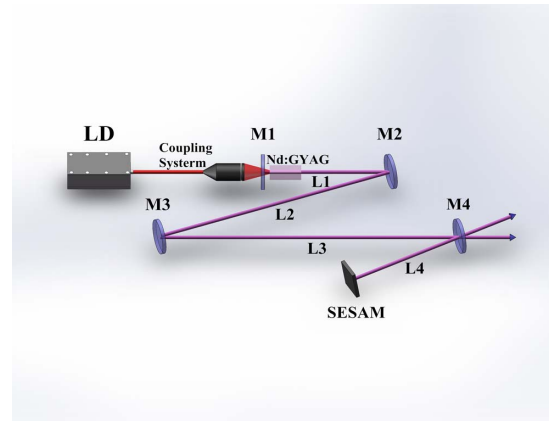Fig. 2. Z-type CWML laser experimental setups.

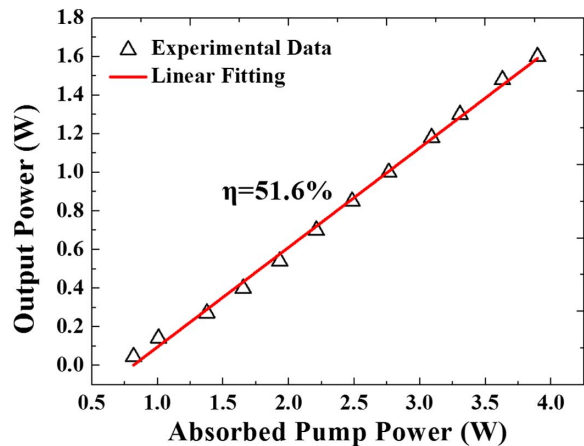Fig. 3. W-type CWML laser experimental setups.

Fig. 4. Function of CW laser output power and the absorbed pump power.

pump power of 3.9 W, corresponding to an optical-to-optical conversion efficiency of 41.0% and a slope efficiency of 51.6%. To protect the laser crystal, the incident pump power was not increased. The central wavelength of the CW laser was measured to be 1064.4 nm with an FWHM of less than 0.1 nm by a commercial spectrum analyzer (AQ 6315A) produced by Yokogawa.

Then, the CWML properties were investigated by a Z-type cavity. The threshold of the laser was about 1.4 W of pump power.

At the beginning, the laser showed Q-switched mode-locked oscillation. Obvious mode-locking pulses inside the Q-switched pulse envelope were observed. The pulse repetition frequency of the Q-switched envelopes increased with the increasing of the incident power. A stable CWML laser was achieved above a 1.8 W absorbed pump power. The laser remained in TEM_{00} mode during the increasing. The laser we got showed a stable CWML laser with 480 mW at 3.2 W absorbed pump power. The relationship between the average output power and absorbed pump power are shown in Fig. 5. The slope efficiency of the laser was about 21.1%. The waveforms of the pulse trace recorded at the scanning times of 10 ns, 20 ns, 200 μs, and 20 ms are shown in Fig. 6.

Smooth and flat waveforms could be clearly observed. The repetition pulse frequency was 113.15 MHz and the pulse width was about 11.1 ps measured by a commercial autocorrelation (AC, Femtochrome Research, Inc. FR-103XL), shown in Fig. 7. The single-pulse energy was calculated to be 4.2 nJ. The central wavelength was about 1064.3 nm with a spectral width of 0.22 nm, which is shown in Fig. 8.

In order to verify the good performance of the Nd:GYAG disordered crystal, another W-type resonator cavity was designed to investigate the CWML laser performance of the GYAG crystal.

After carefully adjusting, the threshold pump power of the mode-locked laser was 1.58 W. The average output power varied with the absorbed pump power, as shown
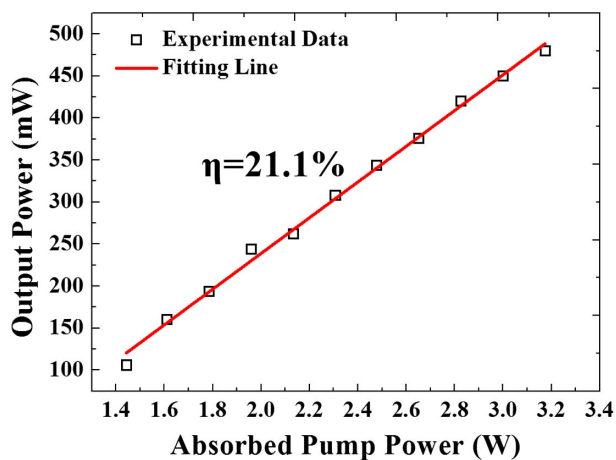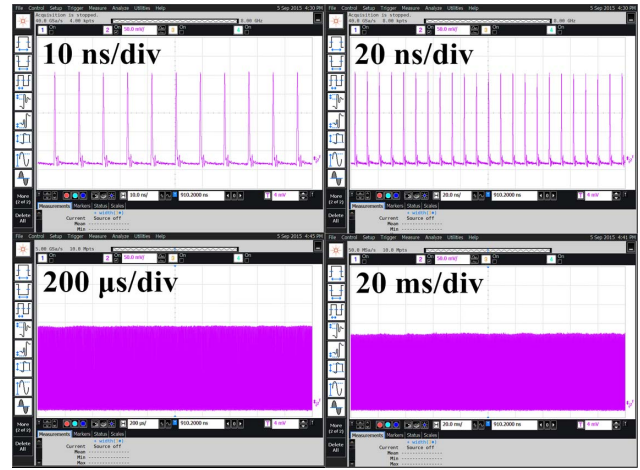

Fig. 6. Z-type cavity CWML laser pulse waveform at scanning times of 10 ns, 20 ns, 200 μs, and 20 ms, respectively.
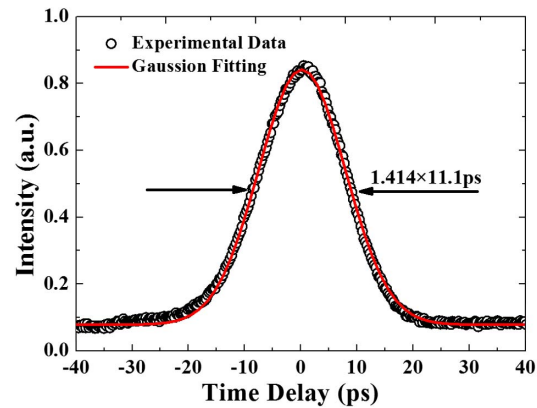

Fig. 7. AC trace of the Z-type mode-locked laser and the fitted result with a Gaussian function.

in Fig. 9. The laser also showed Q-switched mode-locked oscillation. The pulse performance was similar to that of a Z-type laser. A stable CWML laser was achieved above 1.8 W of absorbed pump power. The laser also remained in TEM_{00} mode during the increase. A 210 mW maximum

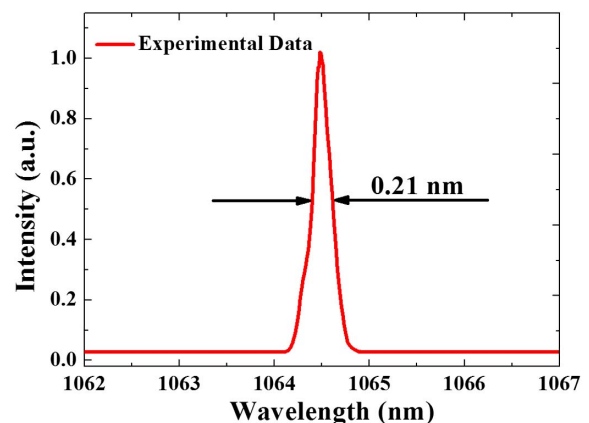Fig. 5. Average output power of the Z-type mode-locked laser change with the 808 nm pump power.

Fig. 8. Spectrum of the Z-type cavity CWML laser.
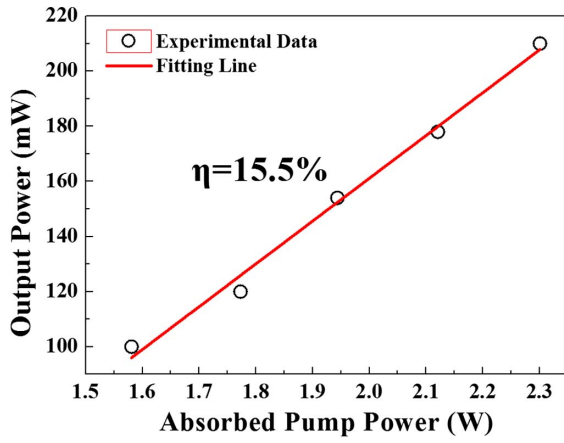
Fig. 9. Average output power of the W-type mode-locked laser change with the 808 nm pump power.

Fig. 10. W-type cavity CWML laser pulse waveform at scanning times of 10 ns, 20 ns, 20 μs, and 10 ms, respectively.

output power was obtained at 2.3 W of absorbed pump power, with a slope efficiency of 15.5% and an optical-to-optical efficiency of 9.1%. Compared with the CW laser, the slope efficiency was lower. This was mainly caused by the saturable absorber SESAM. It is known that the SESAM owns the nonsaturable loss, while the repeated usage may also cause damage to the SESAM surface. This may also cause the loss of energy. Nevertheless, it is clear that the pump power was lower than that of the CW laser and the maximum absorbed pump power was only 2.3 W. A higher incident pump power can also get a higher slope efficiency. Moreover, there might be other factors such as mode-matching, laser reflection angle, and so on that can cause the loss. Because the spot radius at the SESAM was about 50 μm and the transmission of the output coupler was about 4%, the energy density was high enough to damage the saturable absorber. The incident pump power was not increased to prevent the SESAM from damage. Moreover, the waveform of the laser pulses was splitting. In this situation, the waveforms of the CWML laser were recorded at the scanning time of 10 ns, 20 ns, 20 μs, and 10 ms, as were shown in Fig. 10.

It is clear that the waveforms of the mode-locked laser pulses were flat and smooth, which indicated that the single-pulse energies of the CWML laser pulses were nearly equal. This result futher verifies the high stability of the CWML laser. This was mainly because the beam radii of the crystal were small enough, resulting in a higher energy density. The stable mode-locked laser can continuously output more than 24 h. The pulse repetition frequency of the CWML laser was about 88.3 MHz. In this situation, the radio frequency (RF) spectrum was measured via an electrical spectrum analyzer. Figure 11 showed that the signal to noise ratio (SNR) of 88.3 MHz was about 60 dBm, which further verified the stability of the PML pulse.

The optical spectrum of the CWML laser was measured at the same time (Fig. 12). The central wavelength of the CWML laser was 1064.4 nm with a spectral width of 0.286 nm. When the incident pump power decreased,
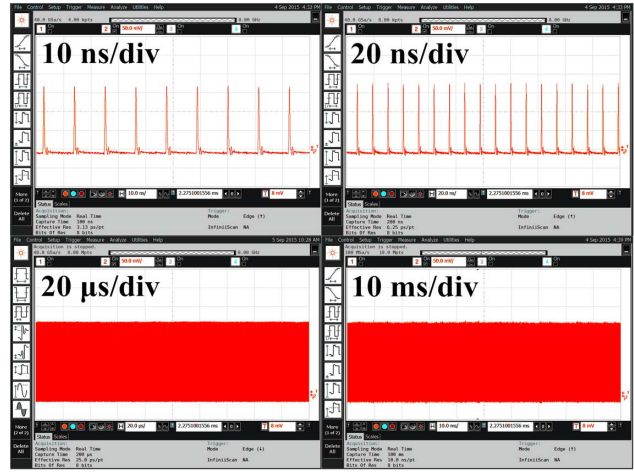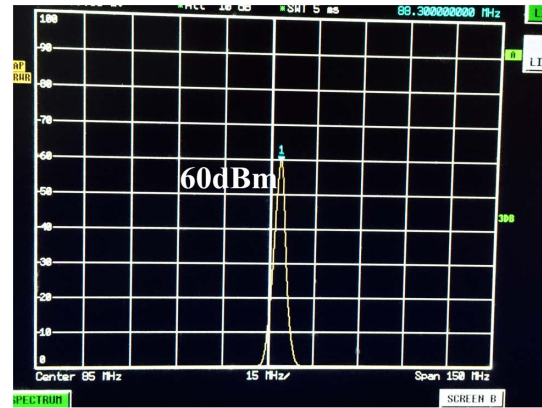

Fig. 11. RF spectrum of the W-type cavity CWML laser.

the pulse widths had no obvious change. By using the same AC to measure the pulse width, mode-locked AC was recorded and is shown in Fig. 13.

According to the AC trace, the pulse width was about 11.1 ps. The time-bandwidth product was about 0.84, which was about twice the limit value. The result
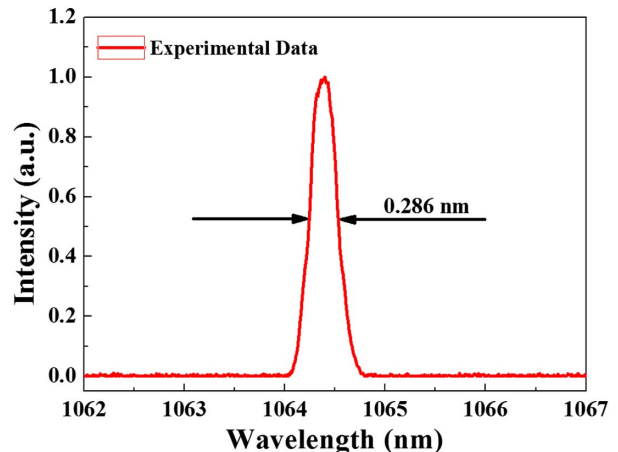

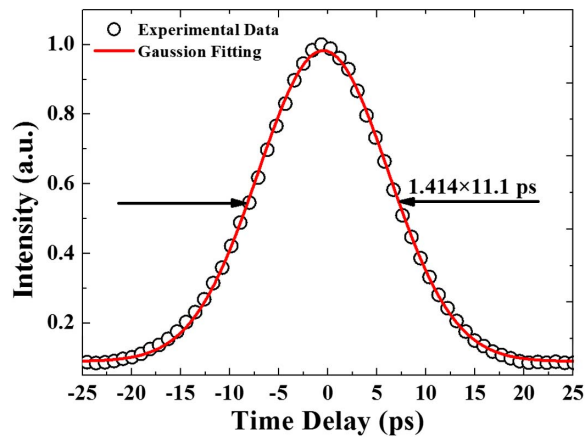Fig. 12. Spectrum of the W-type cavity CWML laser.

Fig. 13. AC trace of the W-type CWML laser and the fitted result with a Gaussian function.

indicated that the CWML laser pulses were slightly chirped. The single-pulse energy and the peak power were 2.4 nJ and 0.2 kW, respectively. Above all, the mode-locked laser was successfully achieved by using Nd:GYAG and an SESAM for the first time.

In conclusion, a stable picosecond CWML Nd:GYAG laser is successfully demonstrated. After employing two different cavities, stable CWML lasers are achieved by both the Z-type cavity and W-type cavity. The 210 mW output power achieved under the 2.3 W absorbed pump power shows a high stability. The excellent optical properties of the Nd:GYAG disordered crystal are necessary for the stable mode-locked laser. We are looking forward to its better performance in the ultrafast laser research field.

References

1. T. Udem, J. Reichert, R. Holzwarth, and T. W. Hansch, Opt. Lett. **24**, 881 (1999).
2. T. Klein, W. Wieser, C. M. Eigenwilling, B. R. Biedemann, and R. Huber, Opt. Express **19**, 3044 (2011).
3. G. R. Jacobovitzveselka, U. Kellerm, and T. Asom, Opt. Lett. **17**, 1791 (1992).
4. F. Chao, L. Jie, W. Yonggang, Z. Lihe, S. Liangbi, and X. Jun, Laser Phys. **23**, 065802 (2013).
5. H. Zhang, S. B. Lu, J. Zheng, J. Du, S. C. Wen, D. Y. Tang, and K. P. Loh, Opt. Express **22**, 7249 (2014).
6. D. Mao, B. Jiang, X. Gan, C. Ma, Y. Chen, C. Zhao, H. Zhang, J. Zheng, and J. Zhao, Photon. Res. **3**, A43 (2015).
7. S. Wang, H. Yu, H. Zhang, A. Wang, M. Zhao, Y. Chen, L. Mei, and J. Wang, Adv. Mater. **26**, 3538 (2014).
8. W. Cai, S. Jiang, S. Xu, Y. Li, J. Liu, C. Li, L. Zheng, L. Su, and J. Xu, Opt. Laser Technol. **65**, 1 (2015).
9. H. Xia, H. Li, C. Lan, C. Li, X. Zhang, S. Zhang, and Y. Liu, Opt. Express **22**, 17341 (2014).
10. H. Zhu, J. Liu, S. Jiang, S. Xu, L. Su, D. Jiang, X. Qian, and J. Xu, **75**, 83 (2015).
11. G. Zhao, J. Hou, Y. Wu, J. He, and X. Hao, Adv. Opt. Mater. **3**, 937 (2015).
12. W. Cai, Q. Peng, W. Hou, J. Liu, and Y. Wang, Opt. Laser Technol. **58**, 194 (2014).
13. D. Mao, S. Zhang, Y. Wang, X. Gan, W. Zhang, T. Mei, Y. Wang, Y. Wang, H. Zeng, and J. Zhao, Opt. Express **23**, 27509 (2015).
14. Q. Yang, D. Liu, J. Liu, Y. Wang, J. Tang, L. Zheng, L. Su, and J. Xu, Opt. Eng. **50**, 114202 (2011).
15. C. Feng, X. Zhang, J. Wang, Z. Liu, Z. Cong, H. Rao, Q. Wang, and J. Fang, Opt. Mater. Express **6**, 1358 (2016).
16. Y. Wang, Z. Qu, J. Liu, and Y. Tsang, J. Lightwave Technol. **30**, 3259 (2012).
17. A. Yoshida, A. Schmidt, V. Petrov, C. Fiebig, G. Erbert, J. Liu, H. Zhang, J. Wang, and U. Griebner, Opt. Lett. **36**, 4425 (2011).
18. U. Keller, K. J. Weingarten, F. X. Kartner, D. Kopf, B. Braun, I. D. Jung, R. Fluck, C. Honninger, N. Matuschek, and J. A. der Au, J. Sel. Top. Quantum Electron. **2**, 435 (1996).
19. L. Guo, W. Hou, H. B. Z, Z. P. Sun, D. Cui, Zu. Y. Xu, Y. G. Wang, and X. Ma, Opt. Express **13**, 4085 (2015).
20. L. J. Qin, D. Y. Tang, G. Q. Xie, H. Luo, C. M. Dong, Z. T. Jia, H. H. Yu, and X. T. Tao, Opt. Commun. **281**, 4762 (2008).
21. X. Wushouer, H. Yu, M. Gong, and P. Yan, Laser Phys. **18**, 1319 (2008).
22. C. Xu, Z. Wei, Y. Zhang, Dehua Li, Z. Zhang, X. Wang, S. Wang, H. J. Eichler, C. Zhang, and C. Gao, Opt. Lett. **34**, 2324 (2009).
23. Y. Sato, J. Saikawa, T. Taira, and A. Ikesue, Opt. Mater. **29**, 1277 (2007).
24. G. B. Lutts, A. L. Denisov, E. V. Zharikov, A. I. Zagumennyi, S. N. Kozlikin, S. V. Lavrishchev, and S. A. Samoylova, Opt. Quantum Electron. **22**, S269 (1990).
25. J. Hou, X. W. Fu, J. L. He, and Y. Yang, IEEE Photon. Technol. Lett. **26**, 40 (2014).
26. J. Q. Di, X. D. Xu, W. D. Tan, J. Zhang, D. Y. Tang, D. Z. Li, D. H. Zhou, F. Wu, and J. Xu, Laser Phys. Lett. **10**, 095801 (2013).
27. G. Q. Xie, D. Y. Tang, H. Luo, H. J. Zhang, H. H. Yu, J. Y. Wang, X. T. Tao, M. H. Jiang, and L. J. Qian, Opt. Lett. **33**, 1872 (2008).
28. A. Agnesi, F. Pirzio, G. Reali, A. Arcangeli, M. Tonelli, Z. Jia, X. Tao, and J. Zhang, Proc. SPIE **7221**, 77210D (2010).
29. H. Luo, D. Y. Tang, G. Q. Xie, W. D. Tan, H. J. Zhang, and H. H. Yu, Opt. Commun. **282**, 291 (2009).
30. Q. Song, G. Wang, B. Zhang, Q. Zhang, W. Wang, M. Wang, G. Sun, Y. Bo, and Q. Peng, Opt. Commun. **347**, 64 (2015).
31. J. Li, P. Gao, L. Zheng, L. Su, J. Xu, and X. Liang, Chin. Opt. Lett. **13**, 011403 (2015).
32. C. Zuo, J. Hou, B. Zhang, and J. He, Chin. Opt. Lett. **13**, 021401 (2015).
33. P. Wang, H. Shi, F. Tan, and P. Wang, Chin. Opt. Lett. **14**, 091405 (2016).
34. J. Q. Di, X. D. Xu, D. Z. Li, D. H. Zhou, F. Wu, Z. W. Zhao, J. Xu, and D. Y. Tang, Laser. Phys. **21**, 1742 (2011).